(2)

NASA
Technical
Paper
2023

AVRADCOM
Technical
Report
82-C-4

October 1982

Analytical and Experimental Investigation of Stator Endwall Contouring in a Small Axial-Flow Turbine

I - Stator Performance

Jeffrey E. Haas

82 11 01 183

NASA

NASA Technical Paper 2023

AVRADCOM Technical Report 82-C-4

1982

Analytical and Experimental Investigation of Stator Endwall Contouring in a Small Axial-Flow Turbine

I - Stator Performance

Jeffrey E. Haas
Propulsion Laboratory
AVRADCOM Research and Technology Laboratories
Lewis Research Center
Cleveland, Ohio

NASA
National Aeronautics and Space Administration
Scientific and Technical Information Branch
1982

Summary

An analytical and experimental investigation of three stator configurations was made to determine the effect of stator outer endwall contouring on stator performance. One of the stator configurations was a cylindrical stator design with an exit tip diameter of 12.77 cm. One contoured stator configuration had an S-shaped outer endwall. The other contoured stator configuration had a conical-convergent outer endwall. The experimental investigation consisted of annular surveys of stator exit total pressure and flow angle for each stator configuration over a range of stator pressure ratio. Radial variations in stator loss and aftermixed flow conditions were obtained. The experimental data were compared with analytical results to assess the validity of the analysis. The experimental data were in good agreement with the analysis.

At design stator pressure ratio the reduction in kinetic energy loss coefficient with contouring was 0.005. More importantly, however, contouring enabled the low-momentum fluid at the tip to be contained in the tip region, which would be expected to significantly improve the flow conditions entering following blade rows. Because of differences in the movement of low-momentum fluid, the radial variations in loss for the three stator configurations showed that the two contoured stators had higher loss near the tip and lower loss near the hub than the cylindrical stator.

The results of the investigation indicated that the amount of loss attributed to secondary flows was nearly constant for the three stator configurations. The reduction in loss with the two contoured stators was attributed to a reduction in boundary layer growth along the vane and endwall surfaces. The stator losses predicted from the analysis for each stator configuration were within 0.022 of those measured. The analysis was able to predict the reduction in loss with the two contoured stators to within 0.002 of that measured. Good agreement with the experimental data was obtained in the radial variation of stator exit flow angle.

Introduction

Axial turbines being designed for advanced high-pressure gas generators in the 1- to 5-kg/sec engine airflow size class are characterized by small blade heights, long chord lengths, and thickened blade profiles. The efficiency levels associated with these small, low-aspect-ratio turbines are low as compared with large turbines, largely because of size effects such as boundary layer thickness, fillet radius, and surface finish and the influence of secondary flows. An important goal of the small turbine research at the NASA Lewis Research Center is to investigate concepts that offer the potential for reducing secondary flows. One concept that has this potential is stator endwall contouring. Contouring the stator endwall reduces the radial and cross-channel pressure gradients and reduces boundary layer growth, thus inhibiting the movement of low-momentum fluid and reducing loss.

The effect of stator endwall contouring was first reported in reference 1. This reference indicated efficiency improvements to 3.5 percent and developed parametric data to optimize contour geometries. Several other investigations have been conducted since the publication of reference 1 to further evaluate the effect of stator contouring. The results from some of these investigations are reported in references 2 to 7. In these programs, reductions in stator kinetic energy loss coefficient ranging from 0.0031 to 0.056 were obtained.

To provide better understanding of the loss mechanisms associated with stator contouring, a program was conducted at Lewis to design and evaluate experimentally and analytically two different contoured stator endwall designs for a 12.77-cm-tip-diameter axial-flow turbine. The first configuration had an S-shaped outer wall profile and was designed by using the parametric data reported in reference 1. The second configuration had a conical-convergent outer wall profile and was designed by simply connecting the stator inlet and exit tip diameters with a straight line. A cylindrical stator was also evaluated to provide a reference.

The test sequence consisted of stator and stage tests. In the stator tests, which are presented in this report, all three stator configurations were evaluated in a cold-air, full-annular cascade environment. Performance was determined from detailed stator exit radial and circumferential surveys of flow angle and total pressure.

This report describes the contoured stator designs, the experimental procedure, the experimental results, and the analytical results. The experimental variations in stator loss and exit flow conditions with circumferential and radial position are presented for the three stator configurations. Also presented are the analytical variations in stator loss and exit flow angle for the three stator configurations. For each stator configuration the analysis was used to calculate a profile loss and an endwall loss.

Symbols

$\bar{e}$	kinetic energy loss coefficient
P	pressure, Pa
R	gas constant, J/kg K
r	radial location, m
T	temperature, K
V	velocity, m/sec
w	mass flow rate, kg/sec

α flow angle measured from axial direction, deg

γ ratio of specific heats

δ ratio of inlet total pressure to U.S. standard sea-level pressure, P_1'/P^*

ϵ function of γ used in relating parameters to those using air inlet conditions at U.S. standard sea-level conditions, $(0.740/\gamma) \times [(\gamma+1)/2]^{\gamma/(\gamma-1)}$

θ_{cr} squared ratio of critical velocity at turbine inlet temperature to critical velocity at U.S. standard sea-level temperature, $(V_{cr}/V_{cr}^*)^2$

ρ density, kg/m^3

Subscripts:

cr flow conditions at Mach 1

fs free stream

id ideal or isentropic

m mean

x axial direction

0 station at turbine inlet (fig. 7)

1 station at stator inlet (fig. 7)

2.5 station 0.52 cm downstream of vane trailing edge (fig. 7)

3M station downstream of vane trailing edge where flow is assumed to be circumferentially uniform (fig. 7)

Superscripts:

$( )'$ total state condition

$( )^*$ U.S. standard sea-level conditions (temperature, 288.15 K; pressure, 101.3 kPa)

$\bar{( )}$ mass-averaged value

Stator Design

In this investigation two different contoured-outer-endwall stator configurations were designed and evaluated to determine their aerodynamic performance. Their performance was compared with that of a reference cylindrical stator configuration, which was the same design reported in reference 8. The cylindrical-endwall stator was designed for a single-stage, axial-flow turbine that had a tip diameter of 12.77 cm, a mass flow rate of about 1 kg/sec, and an inlet temperature and pressure of 1478 K and 9.1 bars absolute, respectively. The stator height was 1.05 cm with an aspect ratio of 0.50 (based on actual chord) and a blade number of 28.

To evaluate the effect of stator endwall contouring, two different contoured-endwall stator configurations were designed. For both configurations the same vane profile shape was used as for the cylindrical stator. The tip sections were extended to define the outer endwall contour shape. The first contoured-endwall stator configuration (designated contoured stator A) had an S-shaped outer wall profile and was designed by using the parametric data reported in reference 1. These data indicated that, for an aspect ratio (based on axial chord) of 0.66, an optimum height ratio (inlet height divided by exit height) of about 1.35 should be chosen.

The second contoured-endwall stator configuration (designated contoured stator B) was designed by using the same inlet and exit tip diameters as contoured stator A. However, instead of an S-shaped curve along the outer endwall, a straight line was used, thereby providing a conical-convergent configuration. Cross-sectional schematics of the three stator configurations are shown in figure 1. The exit vane height for all three configurations was 1.05 cm. For the two contoured-endwall configurations the inlet vane height was 1.42 cm. Table I lists the profile and endwall coordinates for the three stator configurations.

The design blade surface velocities for the three stator configurations are shown in figure 2. These were obtained by using the MERIDL and TSONIC computer codes (refs. 9 and 10). For TSONIC cases with significant supersonic regions the modifications of reference 11 were used. As a result of high solidity, the surface velocity distributions show the stator to be lightly loaded. Except at the tip, the surface velocities were similar for all three stators. At the hub and mean, the surface velocities were slightly lower for the two contoured stators. This was a result of the increased passage height. When the contour geometry for contoured stator A deflected the tip flow radially inward, the surface velocities decreased. This was followed by a large overshoot in the suction-surface velocity. Since all three stator configurations were lightly loaded, the cross-channel pressure gradients were minimized.

The reduction in the cross-channel pressure gradients can be better illustrated by using the blade surface velocities to generate hub and tip endwall pressure contour plots. These are presented in figure 3. Lines of constant static to inlet total pressure ratio are shown along both endwalls for each of the three stator configurations. The blade profiles at the tip section for the two contoured stator configurations appear slightly distorted because the views shown are projections along a meridional length at the tip. For the cylindrical stator (fig. 3(a)) the contour lines are widely spaced through the flow passage along both endwalls and the low-pressure regions extend only a short distance along the suction surface near the trailing edge. These characteristics are indicative of a lightly loaded stator and illustrate the reduced cross-channel pressure gradients. For contoured

stator A (fig. 3(b)) the tip endwall shows no cross-channel pressure contour lines along the first half of the suction surface length. The pressure contour lines become closely spaced nearer the trailing edge and reflect the rapid acceleration along the suction surface that was noted in the discussion of figure 2. For contoured stator B (fig. 3(c)) the pressure contour lines at the tip endwall appear similar to those for the cylindrical stator, except that the contour lines are pushed slightly farther downstream. For all three stator configurations the pressure contour lines are nearly the same at the hub endwall.

Using the velocity distributions of figure 2, analytical pressure distributions along the suction surfaces of the three stator configurations were also obtained. These are plotted in figure 4. Lines of constant static to inlet total pressure ratio are shown. These plots can be used to judge qualitatively how secondary flows on the suction surface will differ among the three stator configurations.

The cylindrical stator (fig. 4(a)) shows pressure contours that have a slight negative slope from hub to tip from the leading edge to about 70 percent of the suction surface length (85 percent of the axial chord length). This negative slope indicates that the pressure along a given radial line would be higher at the hub. Thus low-momentum fluid that forms along the hub wall could migrate radially upward toward the tip. Near the stator exit the contour lines do not extend from hub to tip and the pressure becomes lower near the hub. Therefore the low-momentum fluid that migrated radially upward from the hub as well as low-momentum fluid that formed along the tip wall would migrate to the hub wall.

Contoured stator A (fig. 4(b)) shows pressure contours in the inlet region that extend from hub to tip but change slope near the midspan region. Thus low-momentum fluid along the hub could not migrate radially upward beyond the midspan. At about 60 percent of the suction surface length (80 percent of the axial chord length) there is a low-pressure region near the tip. For this stator the low-momentum fluid at the tip would remain there, causing a loss region. Since the low-momentum fluid at the hub could not migrate radially to the tip, this fluid would remain near the hub.

Contoured stator B (fig. 4(c)) shows pressure contours similar to those for the cylindrical stator. However, the low-pressure region near the stator exit hub is not as severe. For contoured stator B there does not appear to be a strong driving force to cause the low-momentum fluid to be moved to either the hub or the tip. The low-momentum fluid would remain in the area where it was formed. Therefore from these plots it appears that a significant effect of endwall contouring is to reduce the radial migration of low-momentum fluid.

Mean-radius blading information for the cylindrical stator design is shown in figure 5. A stator exit flow angle of 73.5° and a critical velocity ratio of 0.938 are shown. The three stator configurations are shown in figure 6.

Apparatus

The experimental apparatus consisted of the test turbine, the air supply system, and the flow control valves. A cross-sectional view of the test turbine is shown in figure 7. The research rig and a diagram of the test installation are shown in figures 8 and 9, respectively. Dry, pressurized room-temperature air from a central supply system flowed through the test section and was exhausted into the central exhaust system. Pressure control valves at the cascade inlet and exit were used to control the flow conditions upstream and downstream of the test section.

Instrumentation

The station nomenclature and the instrumentation used to measure wall static pressure, total temperature, total pressure, and flow angle are shown in figure 10.

Instrumentation at the turbine inlet (station 0) measured total temperature and total pressure. The temperature was measured with three thermocouple rakes, each containing three thermocouples at the area center radii of three annular areas. A single total pressure probe was located in the center of the pipe.

At the stator inlet (station 1), static pressure and total pressure were measured. Static pressures were obtained from eight taps, with four on the inner wall and four on the outer wall. A radial survey of total pressure was made at one circumferential position by using a shielded (Kiel type) total pressure probe. The sensing tube had an outside diameter of 0.050 cm and a shield diameter of 0.16 cm.

At station 2.5, located 0.52 cm downstream of the vane trailing edge, the static pressure, total pressure, and flow angle were measured. This location corresponded to the plane of the rotor leading edge. Static pressures were again obtained from eight taps, with four on the inner wall and four on the outer wall. Two survey probes were used to determine the radial and circumferential variations in total pressure and flow angle over the vane height and one vane pitch. The two survey probes are shown in figure 11. Two survey probes were required since a single probe could not survey along the entire vane height because of the high endwall curvature of the test hardware. The survey probe shown on the left in figure 11 was used to survey the vane from 20 percent of the vane height to 97.5 percent. The probe was positioned at a fixed angle of 60°, and the total pressure and flow angle were determined from calibration curves.

The survey probe shown on the right in figure 11 was

used to survey the vane from 2.5 percent of the vane height to 20 percent. Because the sensing end of the probe was in line with the probe axis, the probe was used in a self-nulling mode, in which case the probe aligned itself automatically with the direction of flow. Both survey probes were of a three-tube design in which the center tube measured the total pressure and the two side tubes had their sensing ends cut off to form a 90° wedge to measure the flow angle. Each of the stainless steel tubes had an outside diameter of 0.050 cm. The survey probes were inserted into two circumferential slots in the outer casing so that the sensing ends of both probes would be in the plane of station 2.5. During testing the survey regions of the two probes were allowed to overlap in order to verify that good agreement in both measured total pressure and flow angle was obtained.

Procedure

Stator exit radial and circumferential surveys were conducted on the three stator configurations to obtain basic aerodynamic data. The surveys for each configuration were conducted at three stator inlet total to stator exit mean static pressure ratios, nominally, 1.35, 1.8, and 2.1. The tests were conducted at nominal inlet conditions of 300 K and pressures that ranged from 1.3 to 2.1 bars absolute. The inlet pressure was varied to set the stator pressure ratio so that the stator exit tip static pressure would be maintained at about 1 bar absolute.

For each stator configuration and stator pressure ratio, stator exit total pressure and flow angle data were obtained at 15 radii ranging from 2.5 to 97.5 percent of the vane height and over one vane pitch (19.2°) in 20 increments of about 0.65° each. At each discrete point the probe movement was stopped and the probe pressures were allowed to reach equilibrium before data were taken.

A single radial total pressure survey was also made at station 1. The survey was conducted at a stator pressure ratio of 1.8, and data were obtained at several radial positions ranging from about 5 to 95 percent of the inlet vane height.

Data Reduction

The stator kinetic energy loss coefficient was calculated from the stator exit surveys of total pressure and flow angle. In the calculation the static pressure was assumed to vary linearly between the hub and tip wall values.

The calculation of the stator kinetic energy loss coefficient was based on the determination of a hypothetical state where it was assumed that the flow had mixed to a circumferentially uniform condition (station 3M). At each radius the conservation of mass, momentum, and energy was used to obtain this aftermixed state (i.e., $V_{3M,x}$, V_{3M}, T_{3M}, α_{3M}, etc.) from the survey measurements. The calculation procedure is described more fully in reference 12. The aftermixed loss was used herein because it is theoretically independent of the axial location of the survey measurement plane. It should be noted that the aftermixed loss contains not only the stator profile loss, but also the mixing loss. The aftermixed flow conditions can then be directly compared with the stator design velocity diagrams and loss.

The stator aftermixed loss based on kinetic energy can be defined as a function of radius $\bar{e}_{3M}(r)$ or as an overall quantity $\bar{e}_{3M}$ as given by the following equations:

$$\bar{e}_{3M}(r) = 1 - \frac{V_{3M}^2}{V_{3M,id}^2} \tag{1}$$

$$\bar{e}_{3M} = 1 - \frac{\int_{r_h}^{r_t} \rho_{3M} V_{3M,x} V_{3M}^2 r \, dr}{\int_{r_h}^{r_t} \rho_{3M} V_{3M,x} V_{3M,id}^2 r \, dr} \tag{2}$$

where

$$V_{3M,id} = \left\{ \left(\frac{2\gamma}{\gamma - 1} \right) R T_0' \left[1 - \left(\frac{P_{3M}}{P_1'} \right)^{(\gamma-1)/\gamma} \right] \right\}^{1/2} \tag{3}$$

As noted in equation (2) the integrations were performed over the entire stator height. Since the flow measurements were only taken from 2.5 to 97.5 percent of the stator blade height, extrapolations of flow angle and total pressure were made for each pressure ratio and stator configuration. These extrapolations were essentially straight lines, with the total pressure at the endwalls set equal to the wall static pressure.

Results and Discussion

This section presents the aerodynamic data for the three stator configurations. Stator experimental and analytical data are presented in terms of exit flow measurements and overall aftermixed stator loss.

Experimental Results

Mass flow. – The variation of equivalent mass flow with stator pressure ratio is shown in figure 12 for the three stator configurations. For the cylindrical stator the mass flow at design pressure ratio was 5.3 percent larger than design. Most of this increase was due to an oversized throat area. Measurements indicated that the stator throat area was about 7.2 percent larger than that

required to pass design mass flow. The difference (1.9 percent) was attributed to larger than design aerodynamic losses.

The mass flows for contoured stators A and B were 8.9 percent and 4.3 percent larger, respectively, than that for the cylindrical stator. The throat areas for contoured stators A and B were about 9.6 and 4.3 percent larger than the cylindrical stator throat area, respectively. Thus, as compared with the cylindrical stator, the percentage changes in mass flow for the contoured stators were on the average proportional to the increases in throat area. This would indicate that aerodynamic losses for the contoured stators were about the same as that for the cylindrical stator.

Stator inlet total pressure. – Figure 13 shows the radial variation in stator inlet total pressure at a stator pressure ratio of 1.8. The stator inlet total pressure is normalized by the turbine inlet total pressure. The stator inlet total pressure was obtained from a radial survey at one circumferential location by using a shielded (Kiel type) total pressure probe. A shielded total pressure probe was chosen because of its ability to measure a true total pressure over a wide flow angle range. The survey was conducted over a range from about 5 to 95 percent of the stator inlet blade height. Based on the data, the boundary layer height at the hub was less than 5 percent of the blade height, whereas the boundary layer height at the tip was about 10 percent of the blade height. From these data, calculations were made to obtain the displacement and momentum thicknesses on each endwall. These were subsequently used as the initial conditions in the endwall boundary layer analysis.

Aftermixed stator loss. – The radial variation in aftermixed kinetic energy loss coefficient for the three stator configurations is shown in figure 14 at stator pressure ratios of 1.35 and 1.8. The data indicate that at both pressure ratios the cylindrical stator had lower loss near the tip and higher loss near the hub than the two contoured stator configurations. At the design pressure ratio of 1.8, the overall kinetic energy loss coefficients were 0.057, 0.052, and 0.052 for the cylindrical stator, contoured stator A, and contoured stator B, respectively. At the stator pressure ratio of 1.35, the overall loss values were 0.069, 0.062, and 0.061 for the same respective stator configurations.

Although the reductions in loss due to contouring were small, the radial trends shown in figure 14 indicate that the main effect of endwall contouring was to change the radial distribution of loss. For the two contoured stator configurations the loss region remained near the tip instead of migrating radially toward the hub as was the case for the cylindrical stator. The difference in loss distribution should be reflected more noticeably in the stage performance, where the large loss region at the hub for the cylindrical stator may cause detrimental rotor incidence and reaction effects. This type of effect was noted in reference 2, where cascade tests of a cylindrical and a contoured outer endwall stator showed only a 0.002 reduction in loss for the contoured stator, but stage tests indicated a 1.5 point increase in overall stage efficiency. The increase was attributed to improved rotor inlet flow conditions.

Aftermixed flow angle. – The radial variations in aftermixed flow angle at stator pressure ratios of 1.35 and 1.8 are shown in figure 15 for the three stator configurations. At each pressure ratio both contoured stator configurations showed higher turning near the tip, whereas the cylindrical stator had higher turning from the hub to about 50 percent of the blade height. For the pressure ratio of 1.8 the overall, mass-averaged flow angles were 70.8°, 69.7°, and 71.0° for the cylindrical stator, contoured stator A, and contoured stator B, respectively. The lower-than-design, mass-averaged flow angles for the three stator configurations were consistent with the higher-than-design mass flow rates shown in figure 12, although the percentage changes in the cosines of the overall flow angles among the three stator configurations were less than the percentage changes in mass flow. Even though the levels of flow angle may have been in error – a 1° error in an overall flow angle of 70° would account for a 5 percent error in calculating a mass flow – the trends shown in figure 15 are considered accurate.

Mass flux. – Figure 16 shows the radial variation in normalized mass flux for the three stator configurations at a stator pressure ratio of 1.8. The normalized mass flux for each stator configuration is defined as the local product of ρV_x divided by the mass-averaged value ρV_x. The biggest factor in the calculation of ρV_x is the flow angle. From the results of figure 15 it is apparent that there would be a change in the mass flow distribution radially. There was a much higher percentage of the flow near the hub for the two contoured stator configurations and more flow near the tip for the cylindrical stator.

Pressure ratio contours. – Plots of the stator total pressure ratio contours $P'_{2.5}/P'_1$ are shown in figure 17 for the three stator configurations at a stator pressure ratio of 1.8. The contour plots were generated for one vane spacing and over the blade height surveyed. The projection of the trailing edge obtained by using the vane mean camber angle is shown on each plot. All three stator configurations show wide wake regions. All three stators also show loss cores centered at about 30 and 70 percent of the blade height. These loss cores are located on the suction side of the trailing-edge projection and are associated with the boundary layers on both endwalls being deflected across the vane passage, being turned away from the endwalls, and rolling up to form passage vortices in the corners formed by the endwalls and the suction surface. Contoured stators A and B both show

higher loss regions near the tip and smaller loss regions near the hub than the cylindrical stator. This is additional evidence that contouring kept the large loss area near the tip instead of having it migrate radially toward the hub.

Variation of loss with pressure ratio. – The variation of aftermixed stator kinetic energy loss coefficient with stator pressure ratio is shown in figure 18 for the three stator configurations. For each stator configuration, stator exit surveys were conducted at three pressure ratios from about 1.35 to 2.1. For all three configurations the loss coefficient was slightly higher at lower pressure ratios although the variation was less than 0.010. This indicated that the loss was relatively insensitive to Mach number around the design point.

Analytical Results

An important part of this investigation was the application of available analytical methods to the prediction of the losses for the three stator configurations. From these analytical methods, estimates were made of the profile and endwall losses and the radial variation in stator exit flow angle.

The analysis was conducted by using the method discussed in reference 13. Basically, this method couples the three computer codes MERIDL (ref. 9), TSONIC (refs. 10 and 11), and BLAYER (ref. 14) to calculate aftermixed kinetic energy loss coefficients separately for the blade profile and the endwalls. The profile and endwall losses were calculated by using the procedure described in references 12 and 15. The profile loss included the friction loss along the suction and pressure surfaces, the trailing-edge loss, and the mixing loss. The endwall loss was the total friction loss along the hub and tip endwalls up to an axial location corresponding to measuring station 2.5.

Stator loss. – Table II shows the loss breakdown for the three stator configurations at the design stator pressure ratio of 1.8. For each stator the profile and endwall losses were subtracted from the overall measured aftermixed stator loss shown in figure 14. The amount of loss remaining was considered to be secondary flow loss.

The results shown in table II indicate a nearly constant amount of secondary flow loss for all three stators. As noted in the discussion of the design stator surface velocities (fig. 2), all three stator configurations were lightly loaded, thus reducing the cross-channel pressure gradients and subsequently the potential for secondary flow movement. Even though figures 4 and 14 show radial movement of low-momentum fluid, table II indicates that this radial movement did not cause a substantial increase in loss and that endwall contouring changed the secondary flow loss insignificantly. The level of loss was predicted to within 0.015, and the reduction in loss with the two contoured stators was predicted to within 0.001 of that measured. From table II, it can be inferred that the reason for the reduction in loss for the two contoured stator designs was the reduction in boundary layer growth along the profile and endwall surfaces.

The analysis method was also used to calculate the profile loss and the endwall loss for all three stator configurations at stator pressure ratios of 1.35 and 1.95. These results are tabulated in table III along with the results at the design pressure ratio of 1.8. These results are also plotted in figure 19. The experimental data are the same as those shown in figure 18.

The analytical results show total loss values for each stator that are largest at the lowest pressure ratio and remain essentially constant at the two higher pressure ratios. These results are consistent with the trends in the experimental data shown in figure 19. Table III shows that the high loss at the lowest pressure ratio was due primarily to an increase in the profile loss. The profile loss increased because of larger boundary layer growth due to less rapid acceleration along the stator blade surfaces. Table III also shows that the reduction in loss with the two contoured stator configurations was largest at a pressure ratio of 1.35. This trend was also noted with the experimental data and was attributed to the increase in loss for the cylindrical stator at this pressure ratio.

Figure 19 shows that for each stator configuration the difference between the experimental and analytical losses was slightly larger at lower pressure ratios. The difference in loss at pressure ratios of 1.8 and 1.95 was within 0.017, whereas the difference in loss at a pressure ratio of 1.35 was within 0.022. However, the larger difference at the lower pressure ratio is about the same percentage of the overall loss as at the higher pressure ratios. The analytical results predicted the reduction in loss with the two contoured stators within 0.002 of that measured. From the results shown in table III and figure 19, the analytical method provided good agreement with the experimental data in both the levels of loss and the trends in loss.

Stator flow angle. – The radial variations in the analytical flow angles for each stator configuration at pressure ratios of 1.35 and 1.8 are shown in figure 20. These flow angles were obtained by using the MERIDL program (ref. 9). The flow angles are those along a radial midchannel stream surface at an axial location corresponding to station 2.5. Also shown in figure 20 are the experimental aftermixed flow angles that were discussed in connection with figure 15.

At both pressure ratios there was good agreement in the analytical and experimental flow angles. Both the analytical and experimental flow angles show large overturning, particularly at a pressure ratio of 1.35, for the two contoured stator configurations.

Concluding Remarks

The results obtained in this investigation were beneficial for two reasons. First, even though the reduction in loss with contouring was small, the radial redistribution of loss should have a significantly larger effect on stage performance. Second, the analysis method proved to be an accurate means for predicting the reduction in loss with stator endwall contouring. Further validation of this method is desirable. A more meaningful case would be to predict the loss reduction for a much more highly loaded stator configuration in which the radial and cross-channel pressure gradients, and therefore the potential for secondary flows, would be greater.

Summary of Results

An analytical and experimental investigation of three stator configurations was made to evaluate the effect of stator outer endwall contouring on stator performance. One of the stator configurations was a cylindrical endwall design having an exit tip diameter of 12.77 cm. One contoured stator configuration had an S-shaped outer endwall. The other contoured stator configuration had a conical-convergent outer endwall. The experimental investigation consisted of annular surveys of stator exit total pressure and flow angle for each stator configuration over a range of stator pressure ratio. Stator loss and aftermixed flow conditions were varied with radial position. The experimental data were compared with analytical results to assess the validity of the analysis. The results of the investigation are summarized as follows:

1. At design stator pressure ratio the reduction in kinetic energy loss coefficient with contouring was 0.005. More importantly, however, contouring enabled the low-momentum fluid at the tip to be contained in the tip region, and this would be expected to significantly improve the flow conditions entering following blade rows.

2. Because of differences in the movement of low-momentum fluid, the radial variations in loss for the three stator configurations showed that the two contoured stators had higher loss near the tip and lower loss near the hub than the cylindrical stator.

3. The results of the investigation indicated that the amount of loss attributed to secondary flows was nearly constant for the three stator configurations. The reduction in loss with the two contoured stators was attributed to a reduction in the boundary layer growth along the vane and endwall surfaces.

4. The stator losses predicted from the analysis for each stator configuration were within 0.022 of those measured. The analysis was able to predict the reduction in loss with the two contoured stators to within 0.002 of that measured. Good agreement with the experimental data was obtained in the radial variation of stator exit flow angle.

5. The measured mass flows for the two contoured stator configurations were 4.3 and 9.6 percent greater than that for the cylindrical stator, primarily because of differences in the physical throat areas.

Lewis Research Center
National Aeronautics and Space Administration
Cleveland, Ohio, May 17, 1982

References

1. Deich, M. E.; et al.: Method of Increasing the Efficiency of Turbine Stages and Short Blades. Translation No. 2816, Associated Electrical Industries Ltd., England, 1960.
2. Ewen, J. S.; Huber, F. W.; and Mitchell, J. P.: Investigation of the Aerodynamic Performance of Small Axial Turbines. ASME Paper 73-GT-3, Apr. 1973.
3. Due, H. F., Jr.; et al.: Advanced Small Axial Turbine Technology. USAAMRDL-TR-77-1, Teledyne CAE, 1977. (AD-A042517.)
4. Morris, A. W. H.; and Hoare, R. G.: Secondary Loss Measurements in a Cascade of Turbine Blades with Meridional Wall Profiling. ASME Paper 75-WA/GT-13, Nov. 1975.
5. Kopper, F. C.; Milano, R.; and Vanco, M.: An Experimental Investigation of Endwall Profiling in a Turbine Vane Cascade. AIAA Paper 80-1089, June 1980.
6. Okapuu, U.: Some Results from Tests on a High Work Axial Gas Generator Turbine. ASME Paper 74-GT-81, Mar. 1974.
7. Tipton, D. L.: Experimental Investigation of Turbine Endwall Contouring. TDR AX0400-174, Detroit Diesel Allison Technical Data Report, 1981.
8. Haas, Jeffrey E.; and Kofskey, Milton G.: Cold-Air Performance of a 12.766-Centimeter-Tip-Diameter Axial-Flow Cooled Turbine. II - Effect of Air Ejection on Turbine Performance. NASA TP-1018, 1977.
9. Katsanis, Theodore; and McNally, William D.: Revised FORTRAN Program for Calculating Velocities and Streamlines on the Hub-Shroud Midchannel Stream Surface of an Axial-, Radial-, or Mixed-Flow Turbomachine or Annular Duct. Vol. I - User's Manual. NASA TN D-8430, 1977.
10. Katsanis, Theodore: FORTRAN Program for Calculating Transonic Velocities on a Blade-to-Blade Stream Surface of a Turbomachine. NASA TN D-5427, 1969.
11. Wood, Jerry R.: Improved Method for Calculating Transonic Velocities on Blade-to-Blade Stream Surfaces of a Turbomachine. NASA TP-1772, 1981.
12. Goldman, Louis J.; and McLallin, Kerry L.: Cold-Air Annular-Cascade Investigation of Aerodynamic Performance of Cooled Turbine Vanes. I - Facility Description and Base (Solid) Vane Performance. NASA TM X-3006, 1974.
13. Boyle, Robert J.; Rohlik, Harold E.; and Goldman, Louis J.: Analytic Investigation of the Effect of Endwall Contouring on Stator Performance. NASA TP-1943, 1981.
14. McNally, William D.: FORTRAN Program for Calculating

Compressible Laminar and Turbulent Boundary Layers in Arbitrary Pressure Gradients. NASA TN D-5681, 1970.

15. Stewart, Warner L.: Analysis of Two-Dimensional Compressible-Flow Loss Characteristics Downstream of Turbomachine Blade Rows in Terms of Basic Boundary Layer Characteristics. NACA TN-3515, 1955.

TABLE I. - STATOR VANE COORDINATES

(a) Profile coordinates

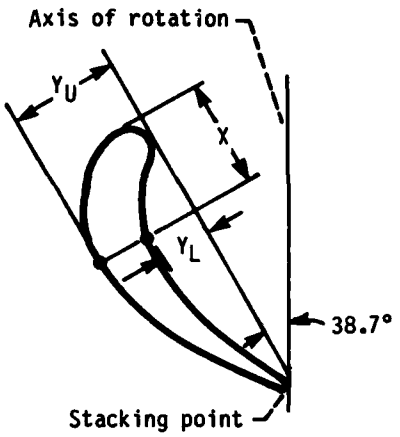

X, cm	Y_L, cm	Y_U, cm
0	0.152	0.152
.102	.009	.377
.203	.009	.502
.305	.080	.590
.406	.153	.652
.508	.218	.692
.610	.274	.713
.711	.318	.719
.813	.347	.713
.914	.363	.697
1.016	.368	.673
1.118	.360	.642
1.219	.344	.604
1.321	.319	.559
1.422	.287	.509
1.524	.249	.452
1.626	.208	.390
1.727	.163	.324
1.829	.116	.253
1.930	.067	.179
2.037	.017	.101
2.103	.030	.030

(b) Endwall coordinates

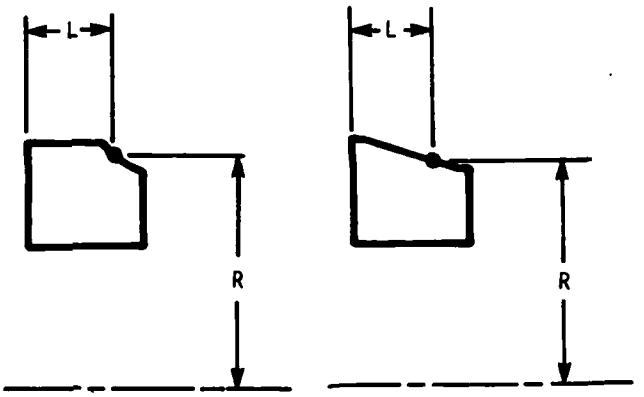

Contoured stator A

L, cm	R, cm
0	6.751
1.016	6.751
1.041	6.749
1.092	6.739
1.143	6.718
1.194	6.675
1.245	6.607
1.295	6.548
1.346	6.502
1.397	6.467
1.448	6.439
1.499	6.416
1.549	6.398
1.600	6.388
1.607	6.383

Contoured stator B

L, cm	R, cm
0	6.751
.025	6.751
.076	6.749
.127	6.739
.152	6.731
.254	6.706
.508	6.642
.767	6.581
1.016	6.518
1.270	6.454
1.501	6.398
1.549	6.388
1.600	6.383
1.607	6.383

TABLE II. - STATOR LOSS BREAKDOWN

[Stator pressure ratio, 1.8.]

	Cylindrical stator	Contoured stator A	Contoured stator B
Overall stator aftermixed loss (measured)	0.057	0.052	0.052
Profile loss	0.025	0.024	0.023
Endwall loss	.017	.014	.015
Secondary flow loss	.015	.014	.014
Total loss	.057	.052	.052

TABLE III. - COMPARISON OF CALCULATED PROFILE AND ENDWALL LOSSES

P_1'/P_{2m}	Loss	Cylindrical stator	Contoured stator A	Contoured stator B
1.35	Profile	0.030	0.026	0.026
	Endwall	.019	.014	.016
	Total	.049	.040	.042
1.8	Profile	0.025	0.024	0.023
	Endwall	.017	.014	.015
	Total	.042	.038	.038
1.95	Profile	0.025	0.023	0.024
	Endwall	.017	.013	.014
	Total	.042	.036	.038

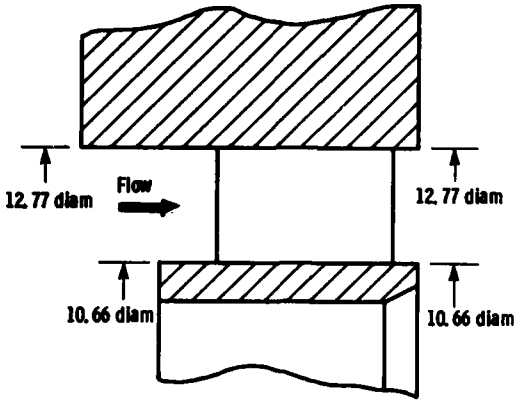

(a) Cylindrical stator.

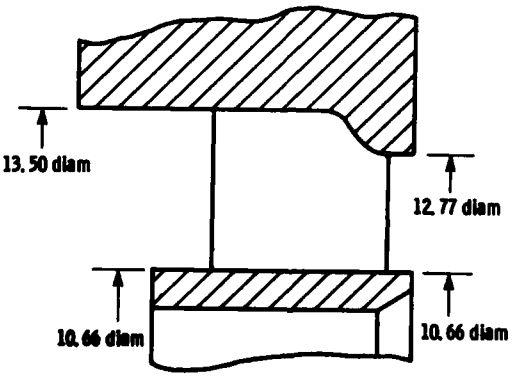

(b) Contoured stator A.

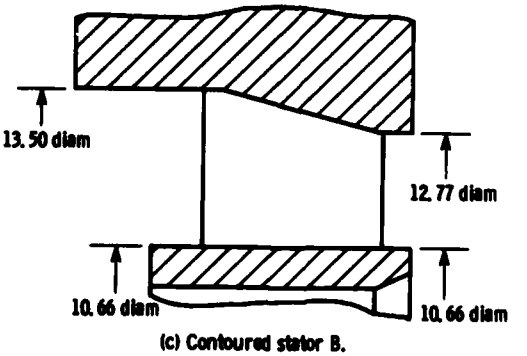

(c) Contoured stator B.

Figure 1. - Schematic cross-sectional view of three stator configurations tested. (Dimensions are in centimeters.)

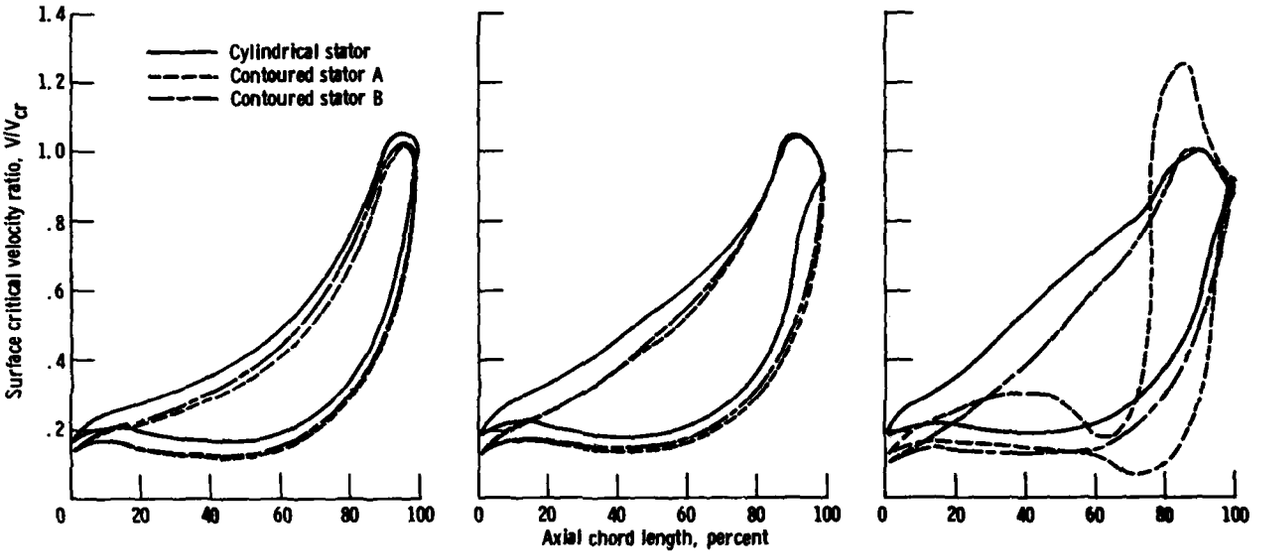

Figure 2. - Design blade surface velocity distributions for the three stator configurations.

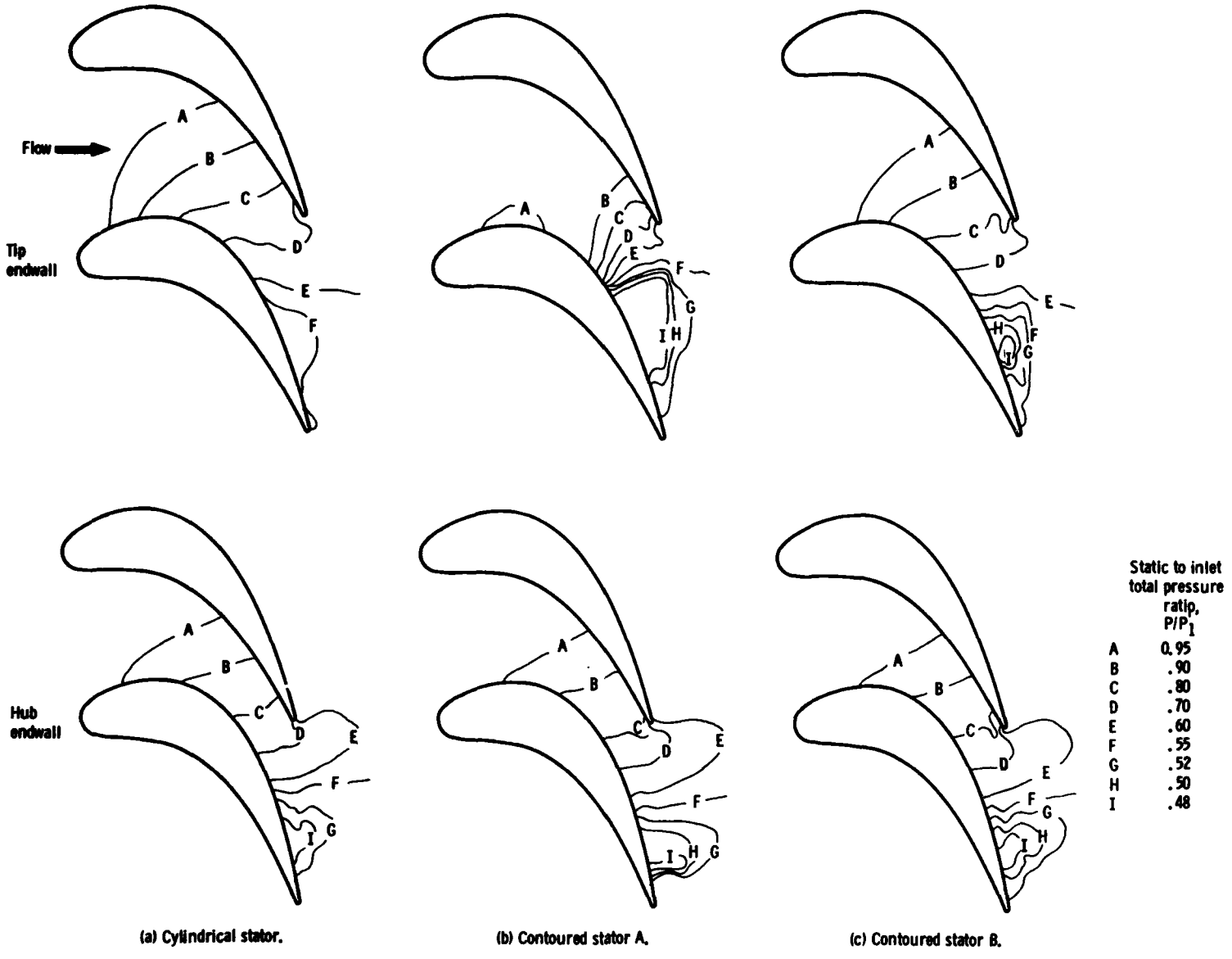

Figure 3. - Comparison of analytical pressure distributions along endwalls of the three stator configurations.

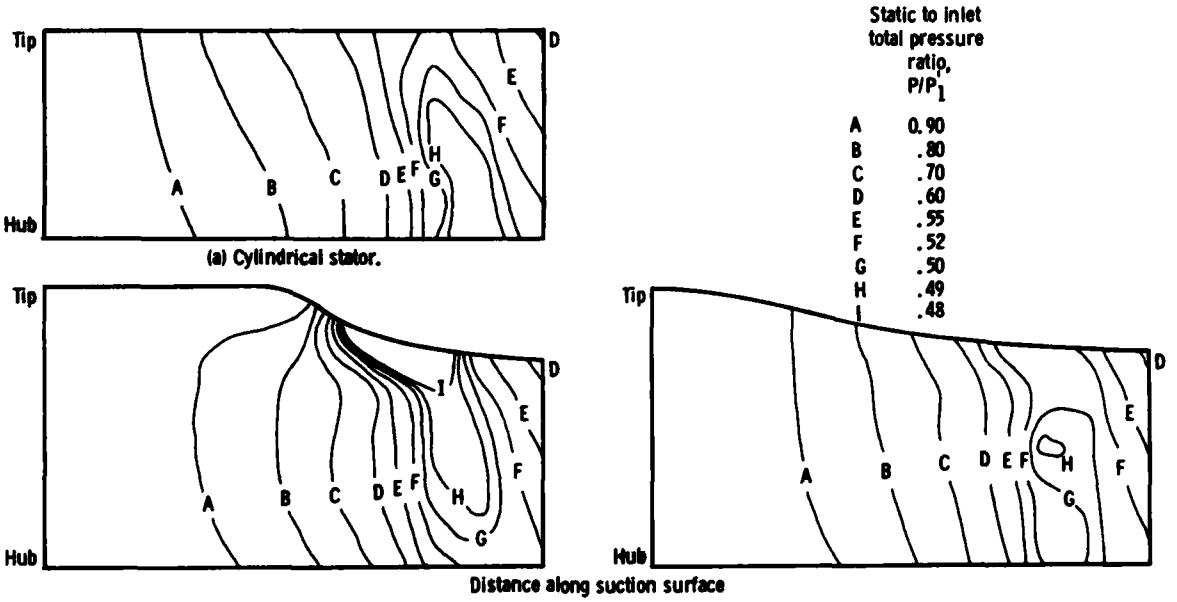

Figure 4. - Comparison of analytical pressure distributions along suction surfaces of the three stator configurations.

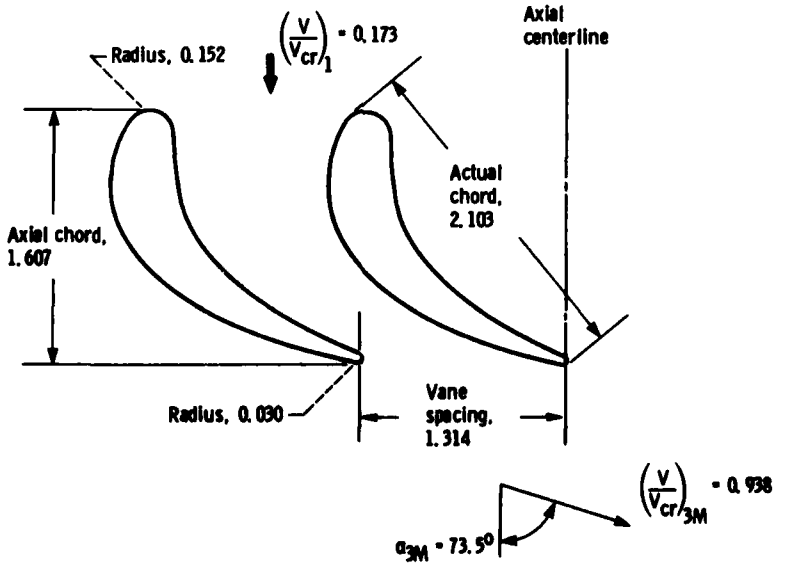

Figure 5. - Mean-radius stator profiles, flow passage, and velocity vectors for cylindrical stator configuration. (Dimensions are in centimeters.)

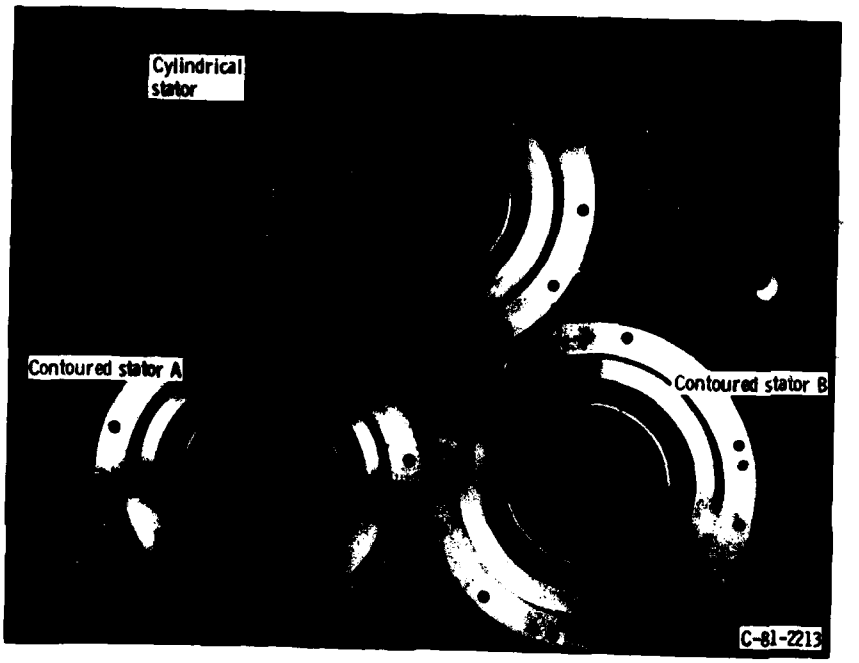

Figure 6. - Stator configurations.

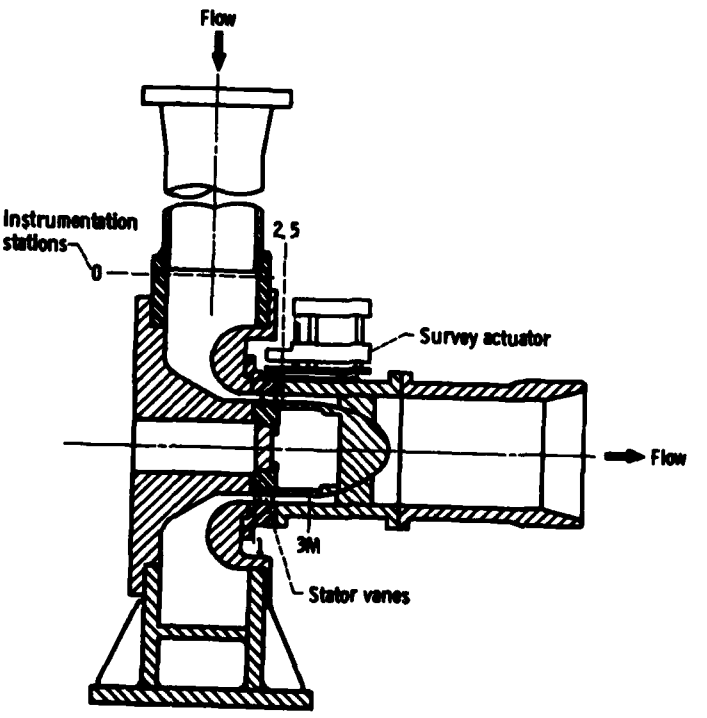

Figure 7. - Schematic cross-sectional view of test turbine.

Figure 8. - Turbine test installation.

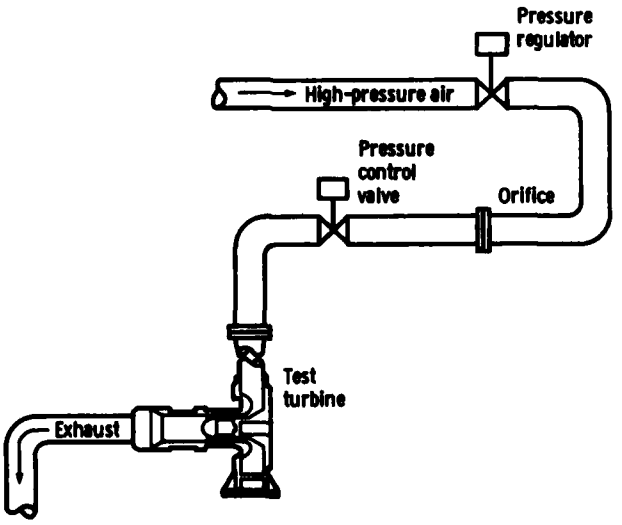

Figure 9. - Test installation diagram.

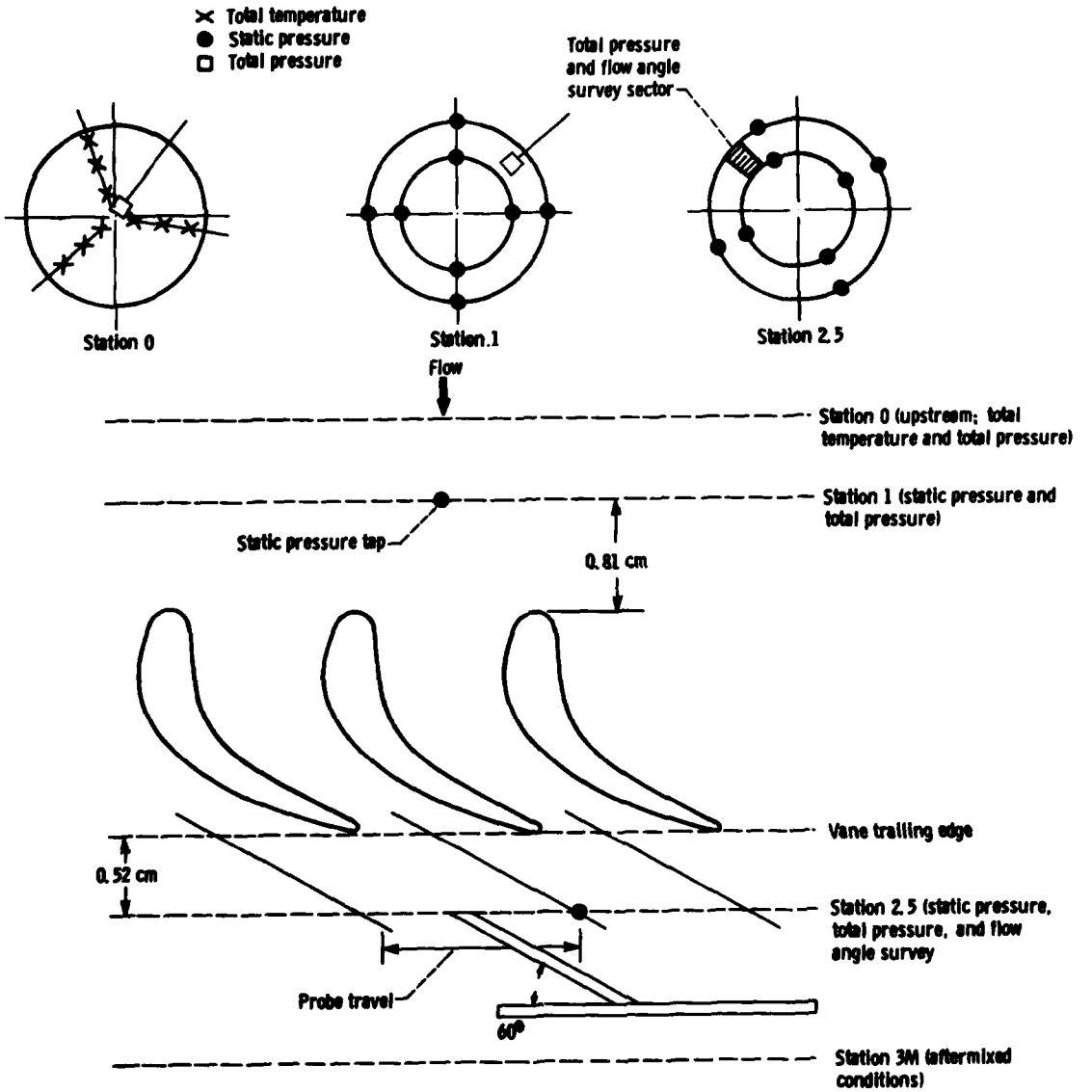

Figure 10. - Flow path instrumentation and station locations.

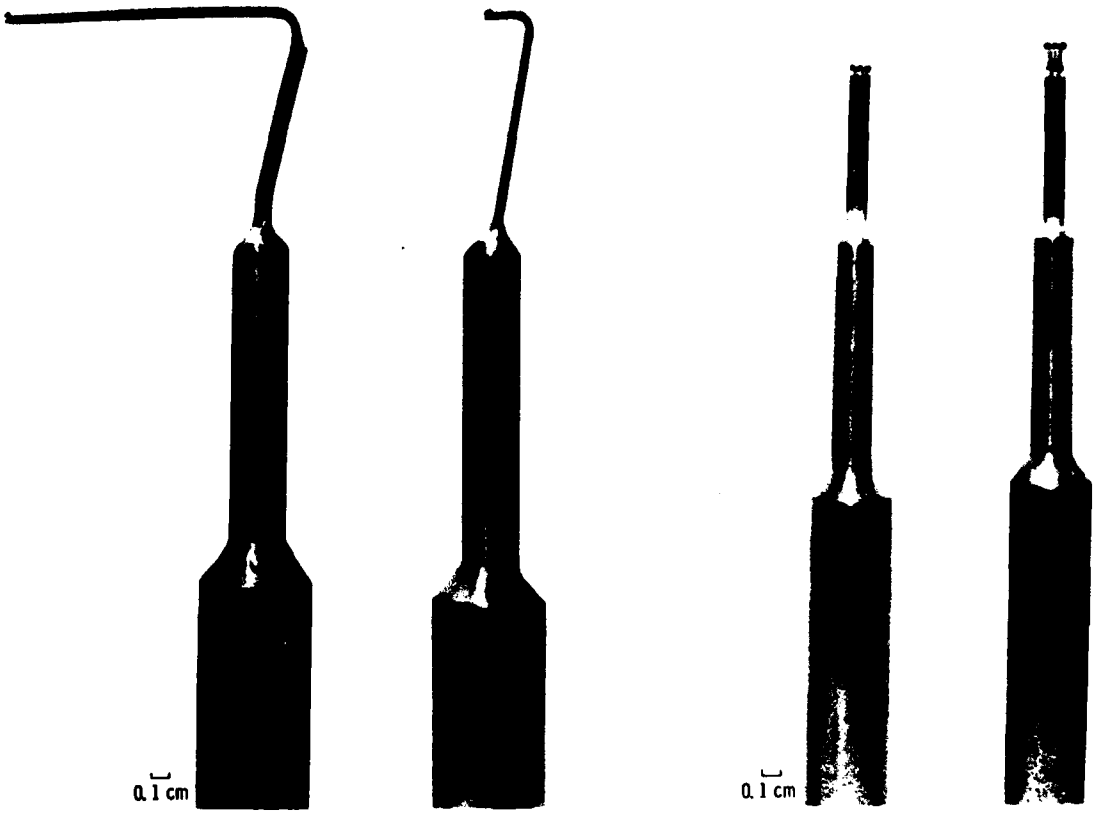

Survey probe used from 2.5 to 20 percent of vane height.

Survey probe used from 20 to 97.5 percent of span vane height.

(a) Side views.

(b) Front views.

Figure 11. - Stator exit survey probes.

C-81-2215

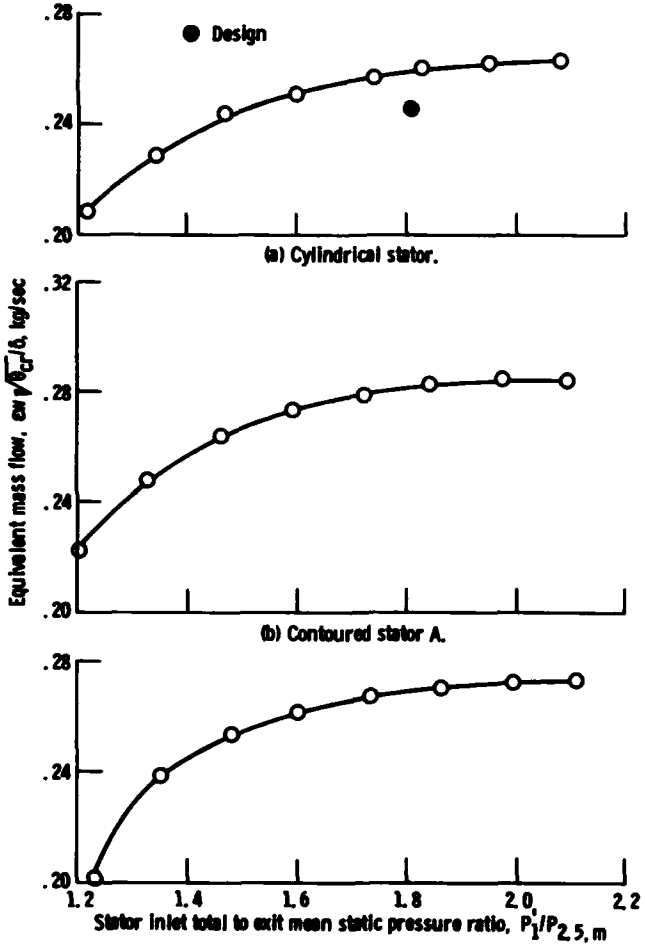

Figure 12. - Variation of mass flow with pressure ratio.

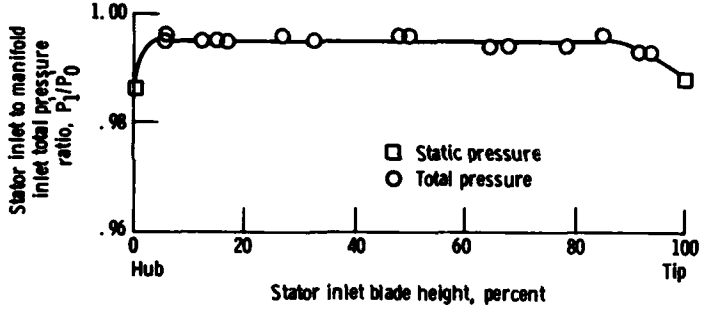

Figure 13. - Radial variation of stator inlet total pressure for a stator pressure ratio of 1.8.

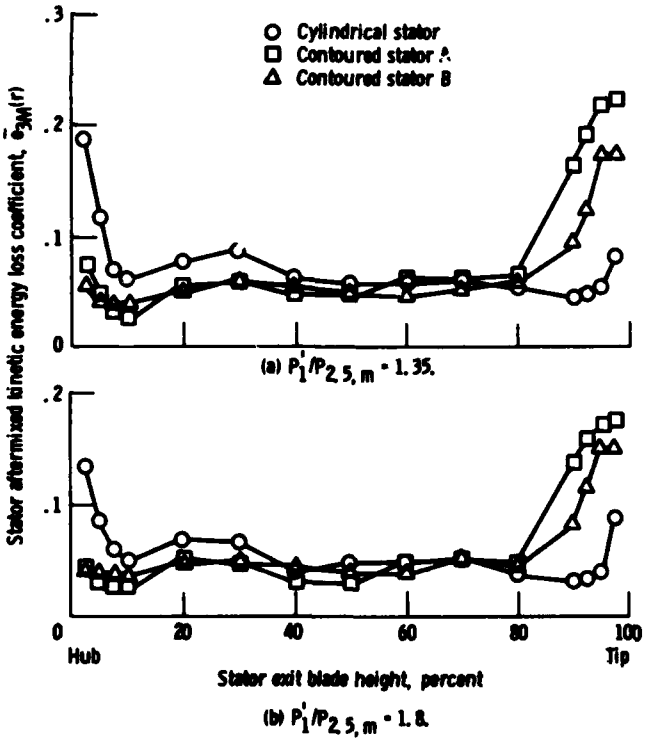

Figure 14. - Radial variation of stator kinetic energy loss coefficient.

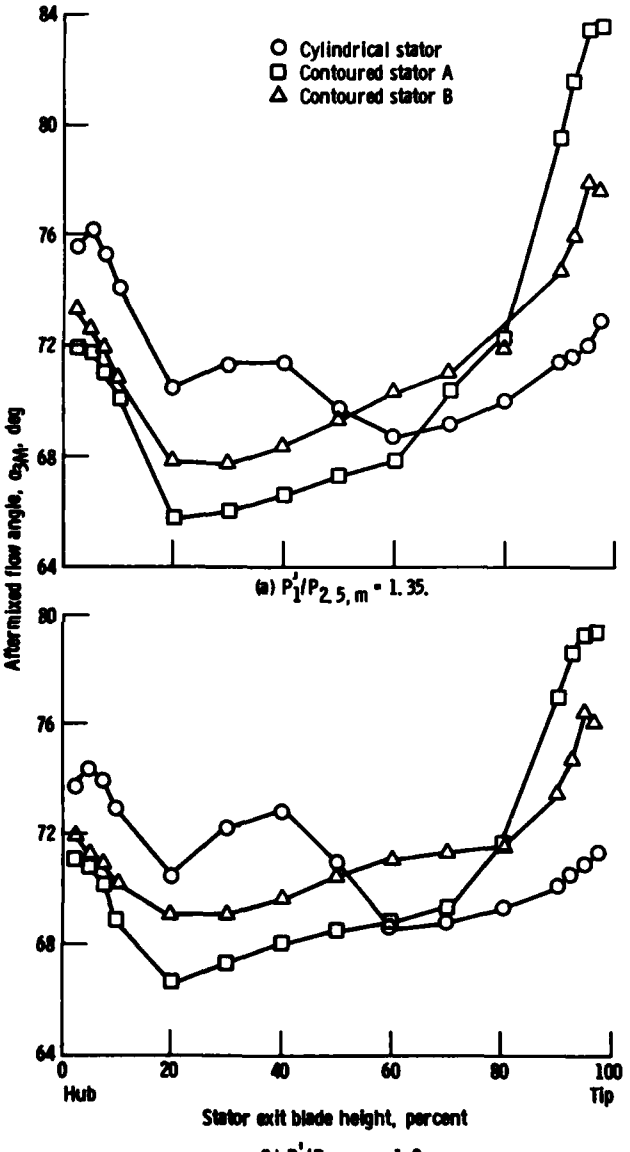

Figure 15. - Radial variation of stator exit flow angle.

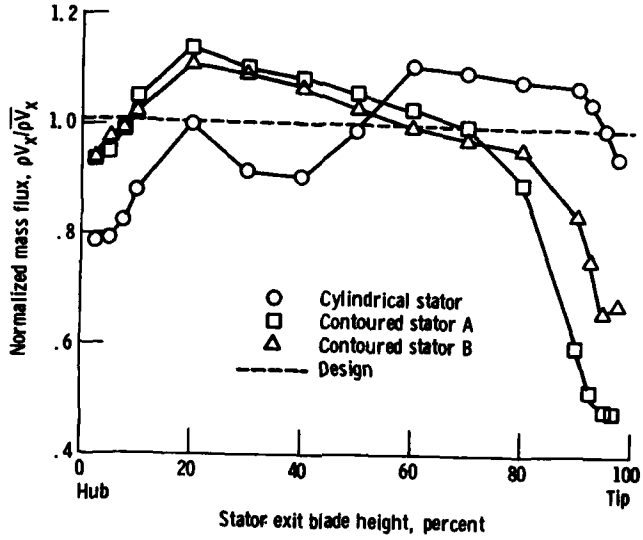

Figure 16. - Radial variation of mass flux at a stator pressure ratio of 1.8.

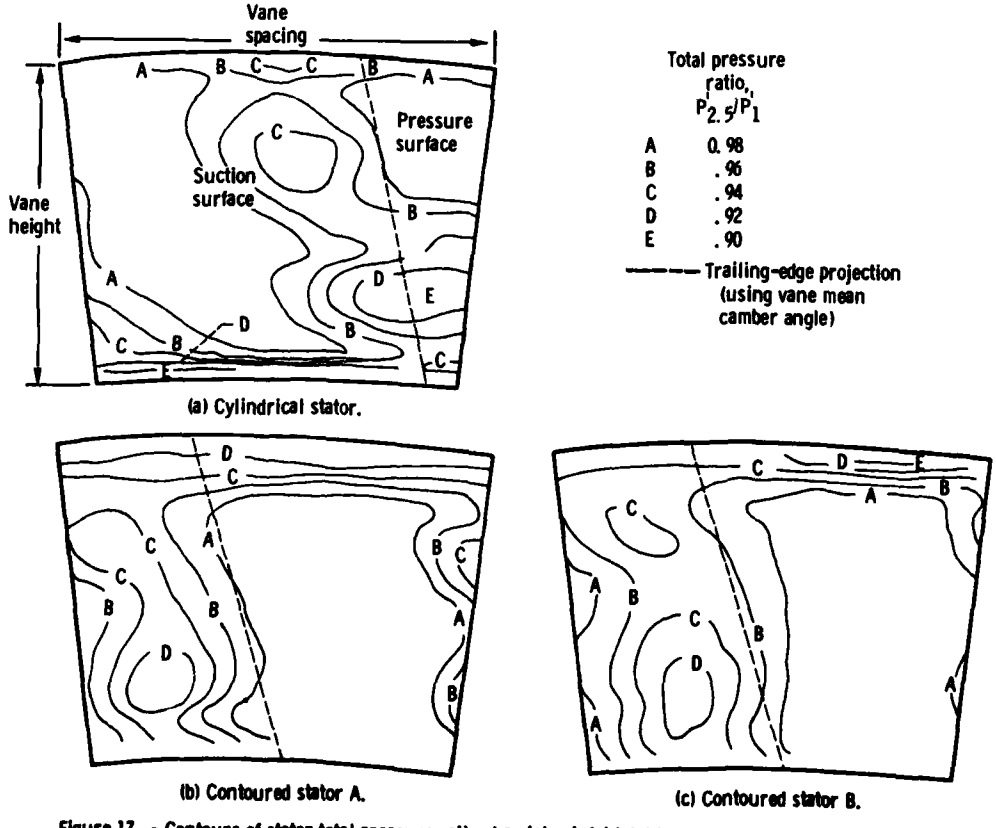

Figure 17. - Contours of stator total pressure ratio at a stator inlet total to exit mean static pressure ratio of 1.8.

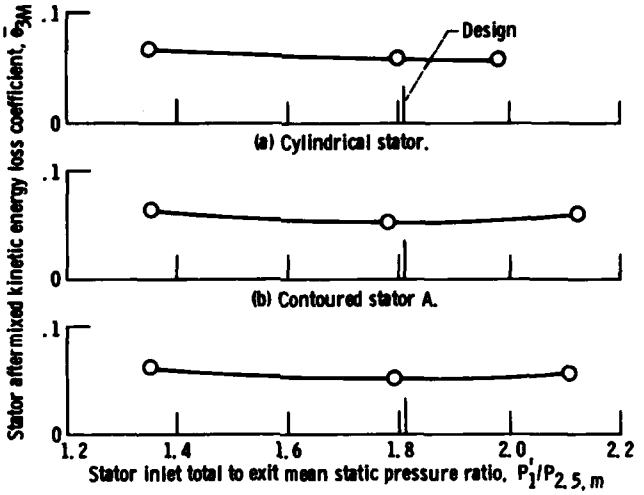

Figure 18. - Variation of stator kinetic energy loss coefficient with pressure ratio.

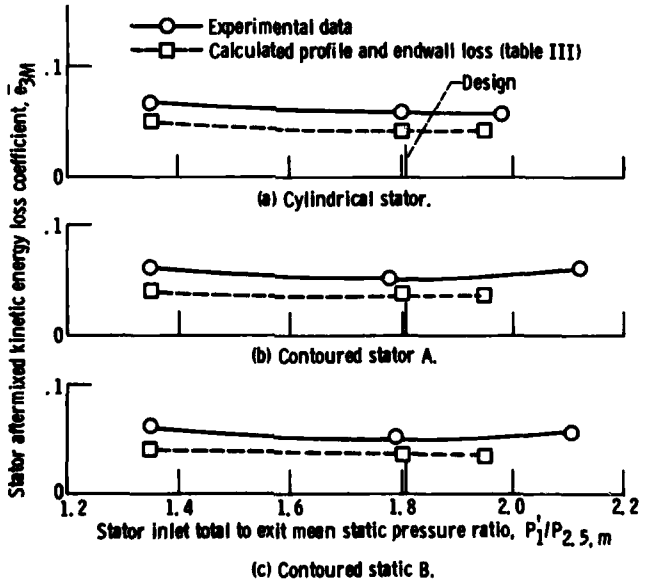

Figure 19. - Variation of stator kinetic energy loss coefficient with pressure ratio - comparison of experimental and calculated results.

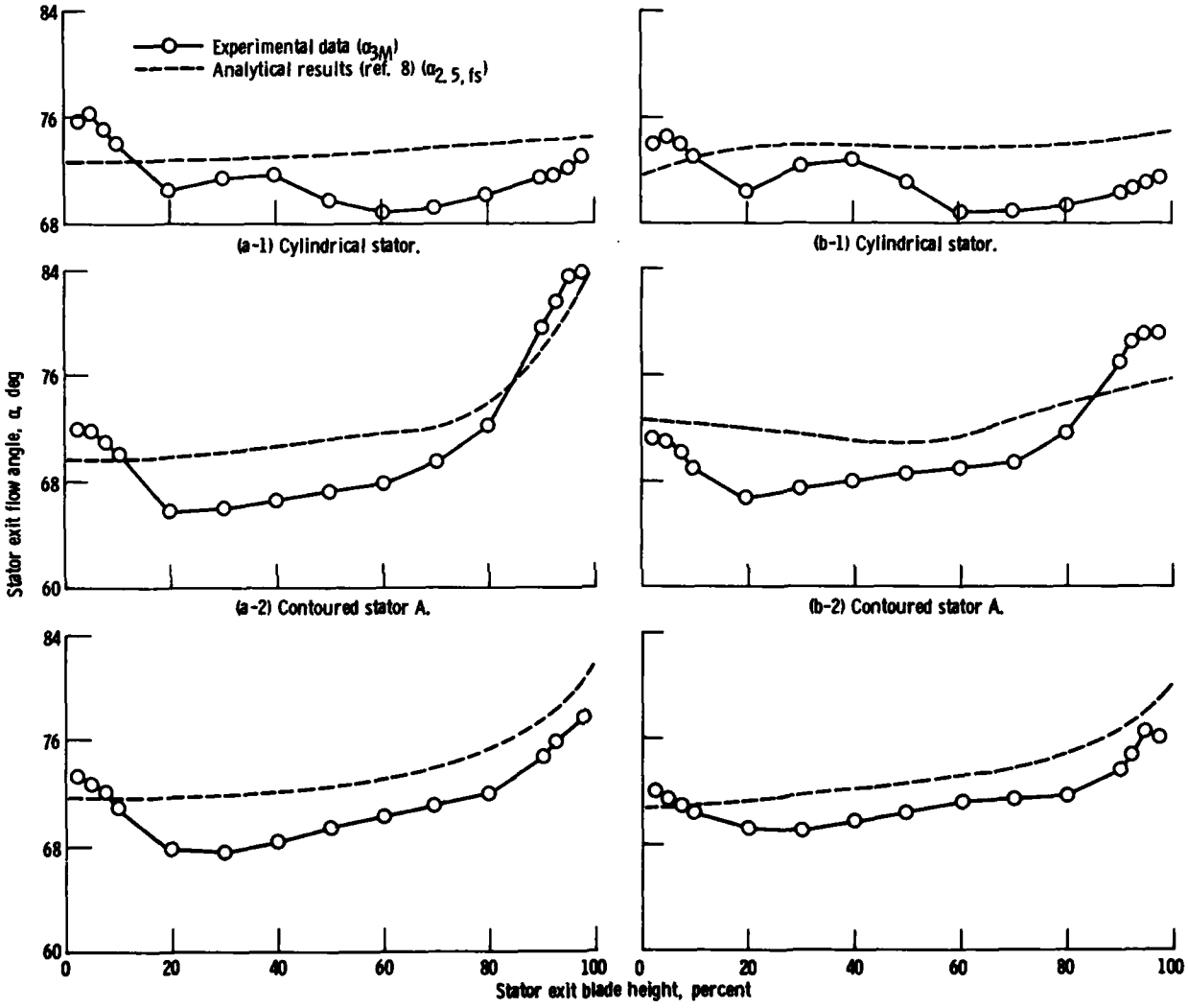

Figure 20. - Comparison of radial variations in measured and calculated stator exit flow angles.

1. Report No. NASA TP-2023 AVRADCOM TR 82-C-4	2. Government Accession No. AD-A120935	3. Recipient's Catalog No.
4. Title and Subtitle ANALYTICAL AND EXPERIMENTAL INVESTIGATION OF STATOR ENDWALL CONTOURING IN A SMALL AXIAL-FLOW TURBINE I - STATOR PERFORMANCE		5. Report Date October 1982 6. Performing Organization Code 505-32-2B
7. Author(s) Jeffrey E. Haas		8. Performing Organization Report No. E-1180 10. Work Unit No.
9. Performing Organization Name and Address NASA Lewis Research Center and AVRADCOM Research and Technology Laboratories Cleveland, Ohio 44135		11. Contract or Grant No.
12. Sponsoring Agency Name and Address National Aeronautics and Space Administration Washington, D.C. 20546 and U.S. Army Aviation Research and Development Command, St. Louis, Mo. 63166		13. Type of Report and Period Covered Technical Paper 14. Sponsoring Agency Code
15. Supplementary Notes		

16. Abstract

An analytical and experimental investigation of three stator configurations was made to determine the effect of stator outer endwall contouring on stator performance. One of the stator configurations was a cylindrical stator design. One contoured stator configuration had an S-shaped outer endwall. The other contoured stator configuration had a conical-convergent outer endwall. The experimental investigation consisted of annular surveys of stator exit total pressure and flow angle for each stator configuration over a range of stator pressure ratio. Radial variations in stator loss and aftermixed flow conditions were obtained. The experimental data were compared with the analytical results to assess the validity of the analysis. The experimental data were in good agreement with the analysis.

17. Key Words (Suggested by Author(s))	18. Distribution Statement
Stator contouring Endwall contouring Axial turbine Stator performance	Unclassified - unlimited STAR Category 07

19. Security Classif. (of this report)	20. Security Classif. (of this page)	21. No. of Pages	22. Price*
Unclassified	Unclassified	24	A02

* For sale by the National Technical Information Service, Springfield, Virginia 22161

NASA-Langley, 1982